Eur Biophys J (2011) 40:1371–1381
DOI 10.1007/s00249-011-0720-5

ORIGINAL PAPER

EBSA
Biophysics in Europe

Characterizing weak protein–protein complexes by NMR residual dipolar couplings

Malene Ringkjøbing Jensen · Jose-Luis Ortega-Roldan · Loïc Salmon · Nico van Nuland · Martin Blackledge

Received: 26 March 2011 / Revised: 27 May 2011 / Accepted: 1 June 2011 / Published online: 28 June 2011

Abstract Protein–protein interactions occur with a wide range of affinities from tight complexes characterized by femtomolar dissociation constants to weak, and more transient, complexes of millimolar affinity. Many of the weak and transiently formed protein–protein complexes have escaped characterization due to the difficulties in obtaining experimental parameters that report on the complexes alone without contributions from the unbound, free proteins. Here, we review recent developments for characterizing the structures of weak protein–protein complexes using nuclear magnetic resonance spectroscopy with special emphasis on the utility of residual dipolar couplings.

Keywords NMR · Interaction · Protein · Dynamics · Structure · Complex

Special Issue: Transient interactions in biology.

M. R. Jensen · L. Salmon · M. Blackledge (✉)
Protein Dynamics and Flexibility, Institut de Biologie Structurale Jean-Pierre Ebel, CEA-CNRS-UJF UMR 5075, 41 Rue Jules Horowitz, 38027 Grenoble, France
e-mail: martin.blackledge@ibs.fr

J.-L. Ortega-Roldan
Department of Biochemistry, University of Oxford, South Parks Road, Oxford OX1 3QU, UK

N. van Nuland
Structural Biology Brussels, VIB Department of Molecular and Cellular Interactions, Vrije Universiteit Brussel, Pleinlaan 2, 1050 Brussel, Belgium

Introduction

Protein–protein interactions occur with a wide range of affinities from tight complexes characterized by femtomolar dissociation constants to weak, and more transient, complexes of millimolar affinity. In recent years, it has become clear that even weak protein–protein interactions play key roles in a vast range of biological processes where reversibility is an important factor, such as cell signaling, electron transport, transcription and replication, and rapid enzyme catalysis. The structural characterization of weak protein–protein complexes is, however, associated with a number of technical difficulties, in particular with finding experimental conditions where structural parameters can be measured from the complex alone without interference from the free forms of the proteins. For these reasons, X-ray crystallography, the most powerful technique for determining high-resolution structures of protein–protein complexes, finds its limitations when considering low affinity complexes.

Nuclear magnetic resonance (NMR) spectroscopy is uniquely suited for studying weak protein–protein interactions at atomic resolution (Zuiderweg 2002; Vaynberg and Qin 2006; Takeuchi and Wagner 2006; Fielding 2007; O'Connell et al. 2009). NMR allows a determination of the dissociation constant from the chemical shift changes induced by complex formation and a mapping of the interface between the two proteins of the complex. In addition, residual dipolar couplings (RDCs), measured under partial alignment of the protein molecules in the magnetic field, are particularly powerful as they report not only on the structure of the individual proteins, but also on the orientation of the two partners with respect to a common alignment frame (the alignment tensor) (Tjandra and Bax 1997; Bax 2003; Bax and Grishaev 2005). This of

course requires that the RDCs have been measured for each of the two proteins under saturating conditions where the molar fraction, p_{bound}, of the protein in the complex is almost equal to 1. For weak complexes of micro- to millimolar affinity, it is usually not possibly to reach saturation directly for any of the two partners without using excessively high protein concentrations.

This review describes the structural characterization of weak protein–protein complexes using RDCs as orientational restraints with special emphasis on how to overcome the saturation problem and obtain RDCs that emanate from the complex alone. As an example, we will focus on a recent NMR study characterizing the weak interaction between the protein ubiquitin and the third SH3 domain of the CD2-associated protein (SH3-C) (Ortega Roldan et al. 2007, 2009). Ubiquitin regulates a wide variety of cellular activities ranging from transcriptional regulation to cell signaling and membrane trafficking, while SH3 domains constitute a highly conserved protein family where the amino acid composition only differs at a few key sites and thereby allows for a wide range of molecular targets. Complexes formed between ubiquitin and SH3 domains are particularly interesting because ubiquitin does not contain the proline-rich motif that normally characterizes the interaction partners of SH3 domains. Nevertheless, it has been shown that the ubiquitin binding surface of the SH3 domains overlaps largely with the canonical binding surface for proline-rich ligands suggesting that ubiquitin can negatively regulate interaction of SH3 domains with molecular targets (Stamenova et al. 2007).

Determination of complex dissociation constants by NMR

Dissociation constants of protein–protein complexes are usually obtained by measuring the chemical shift perturbations in a ^{15}N-labeled protein upon titration with known quantities of its unlabeled partner and vice versa. To increase the accuracy of the determination of the dissociation constant, the chemical shift perturbations, $\Delta\delta$, of several peaks as a function of the applied protein concentrations can be fitted simultaneously to obtain a single dissociation constant according to:

$$\Delta\delta = \frac{(\delta_{bound} - \delta_{free})}{2P}\left[P + L + K_D - \sqrt{(P + L + K_D)^2 - 4PL}\right] \quad (1)$$

Here (δ_{bound}–δ_{free}) is the chemical shift difference between the free and the bound (complex) forms, K_D is the dissociation constant, and P and L are the total concentrations of the ^{15}N-labeled protein and the unlabeled partner protein (ligand), respectively. The use of Eq. 1 requires that the two proteins form a 1:1 complex and that the complex formation occurs within the so-called fast exchange regime, where the exchange rate, k_{ex}, between free and bound forms is much faster than the chemical shift difference between the two forms. Usually this exchange regime manifests itself by the absence of significant line broadening of the shifted resonances during the course of the titration.

In the case of the ubiquitin/SH3-C complex, the K_D value was determined from the resonances that undergo the largest chemical shift perturbations in the ^{1}H–^{15}N HSQC spectra upon addition of the unlabeled partner protein (Fig. 1). The line widths of the resonances in the HSQC spectra of both SH3-C and ubiquitin do not change during the titrations indicating that the complex formation falls within the fast exchange regime (Fig. 1a, b). A simultaneous fit of Eq. 1 using shifting peaks from the two complementary titrations yielded a K_D value of 132 ± 13 μM corresponding to the formation of a weak complex (Fig. 1c, d). It is worth noting that in this case saturation of either protein has not been reached even for 1:4 molar ratios showing that the complex cannot easily be isolated under the experimental conditions used for the NMR experiments.

Mapping the intermolecular interface of protein complexes by NMR

If a specific complex is formed between two proteins, the chemical shift perturbations measured in the two complementary titration experiments map to specific regions of the two proteins. Residues in these regions are either at or near the binding sites or involved in structural rearrangements upon partner protein binding. For the ubiquitin/SH3-C complex, the interface between the two proteins involves the RT loop (residues 18–23), the nSrc loop (residues 37–39), the beginning of the β-III strand (residues 42–44), and residues 54–58 of SH3-C and two typical binding regions of ubiquitin, namely that of Ile44 and Gly76 (Fig. 2a, b). The regions of SH3-C and ubiquitin involved in the interaction cluster on the surface of the two proteins (Fig. 2c, d) and constitute the interface of the complex. Chemical shift perturbations alone are usually not sufficient to determine the structure of the complex, however, they can provide an ensemble of possible conformations of the complex, for example through the use of the program HADDOCK (Dominguez et al. 2003), which uses as input chemical shift perturbations converted into ambiguous intermolecular distance restraints (AIRs). From the results of the HADDOCK calculation on the basis of chemical shift data alone (Fig. 3a), it is clear that orientational

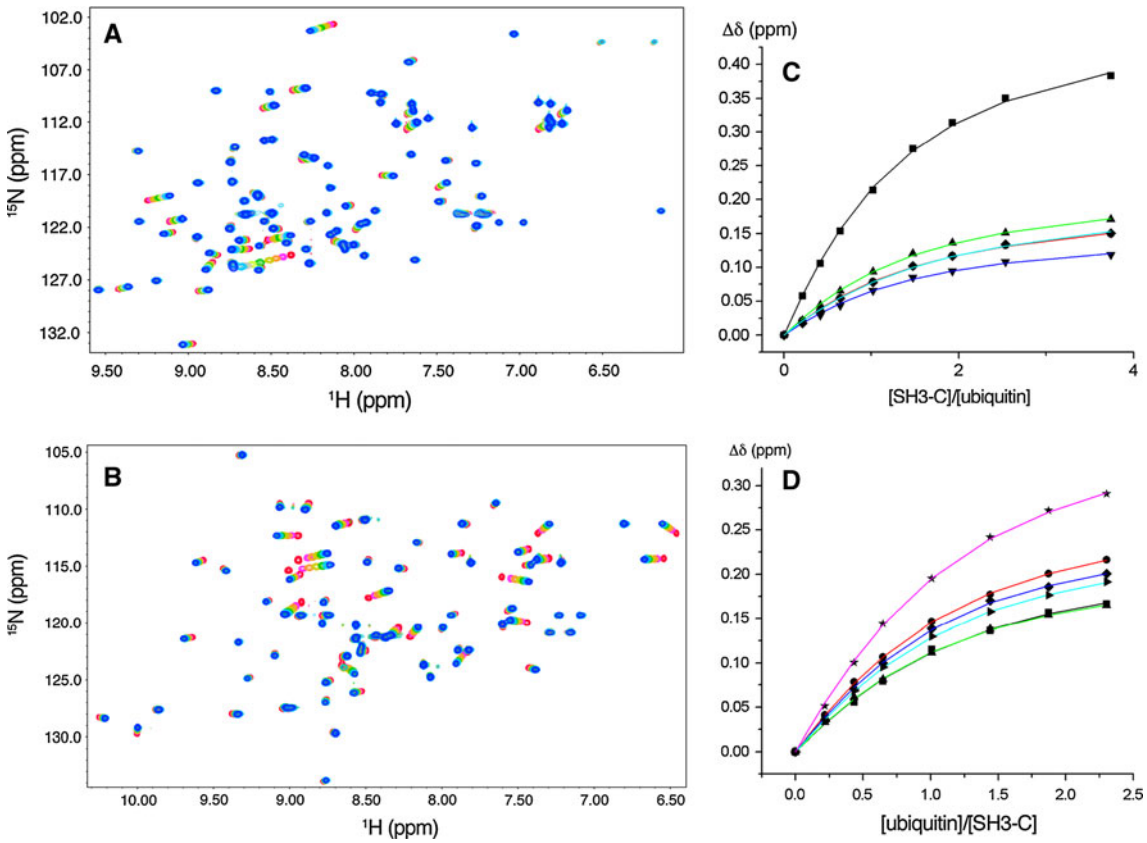

Fig. 1a–d Determination of the dissociation constant of the ubiquitin/SH3-C complex. **a** Chemical shift perturbations in the ^{1}H–^{15}N HSQC spectrum of ubiquitin upon addition of increasing amounts of unlabeled SH3-C. **b** Chemical shift perturbations in the ^{1}H–^{15}N HSQC spectrum of SH3-C upon addition of increasing amounts of unlabeled ubiquitin. **c** Determination of the dissociation constant from a simultaneous fit of selected residues in ubiquitin: R42 (*cyan*), F45 (*blue*), G47 (*green*), H68 (*red*), and L73 (*black*). **d** Determination of the dissociation constant from a simultaneous fit of selected residues in SH3-C: T18 (*magenta*), N19 (*cyan*), E20 (*blue*), D21 (*green*), T38 (*red*), and W44 (*black*)

restraints are needed to refine the relative position of the two proteins in the ubiquitin/SH3-C complex.

Residual dipolar couplings as orientational restraints

The dipolar coupling D_{ij} between two spins i and j is given by (Emsley and Lindon 1975):

$$D_{ij} = -\frac{\gamma_i \gamma_j \hbar \mu_0}{8\pi^2 r^3} \left\langle \frac{3\cos^2 \Omega - 1}{2} \right\rangle \quad (2)$$

Here, γ_i and γ_j are the gyromagnetic ratios of spin i and j, respectively, Ω is the angle of the internuclear vector with the direction of the static magnetic field, and r is the internuclear distance. The brackets in the equation indicate an average over all conformations sampled on time scales faster than the millisecond. The dipolar coupling between two nuclei is effectively averaged to zero in solution NMR because all orientations of the protein molecule are equally probable in an isotropic solution. A small part of the dipolar coupling can be reintroduced by partially aligning the molecules in the magnetic field, for example using an anisotropic solution (Tjandra and Bax 1997) or exploiting the magnetic anisotropy of paramagnetic metal ions (Tolman et al. 1995). These so-called residual dipolar couplings (RDCs) add to the experimentally measured scalar couplings (J-couplings) allowing RDCs to be extracted as the difference in couplings in the NMR spectra obtained in isotropic and anisotropic solutions, respectively. A number of anisotropic media have been proposed for weakly aligning protein molecules in the magnetic field by exploiting steric repulsion between the protein and the medium or from a combination of electrostatic and steric interactions. Among the most common alignment media are filamentous phages (Hansen et al. 1998; Clore et al. 1998; Torbet and Maret 1979), lipid bicelles (Tjandra and Bax 1997), ethylene glycol/alcohol phases (Rückert and Otting 2000), and polyacrylamide gels that can be strained either laterally or longitudinally to produce anisotropic cavities (Sass et al. 2000; Tycko et al. 2000). Choosing an appropriate alignment medium depends first of all on the experimental conditions such as buffer, pH, and

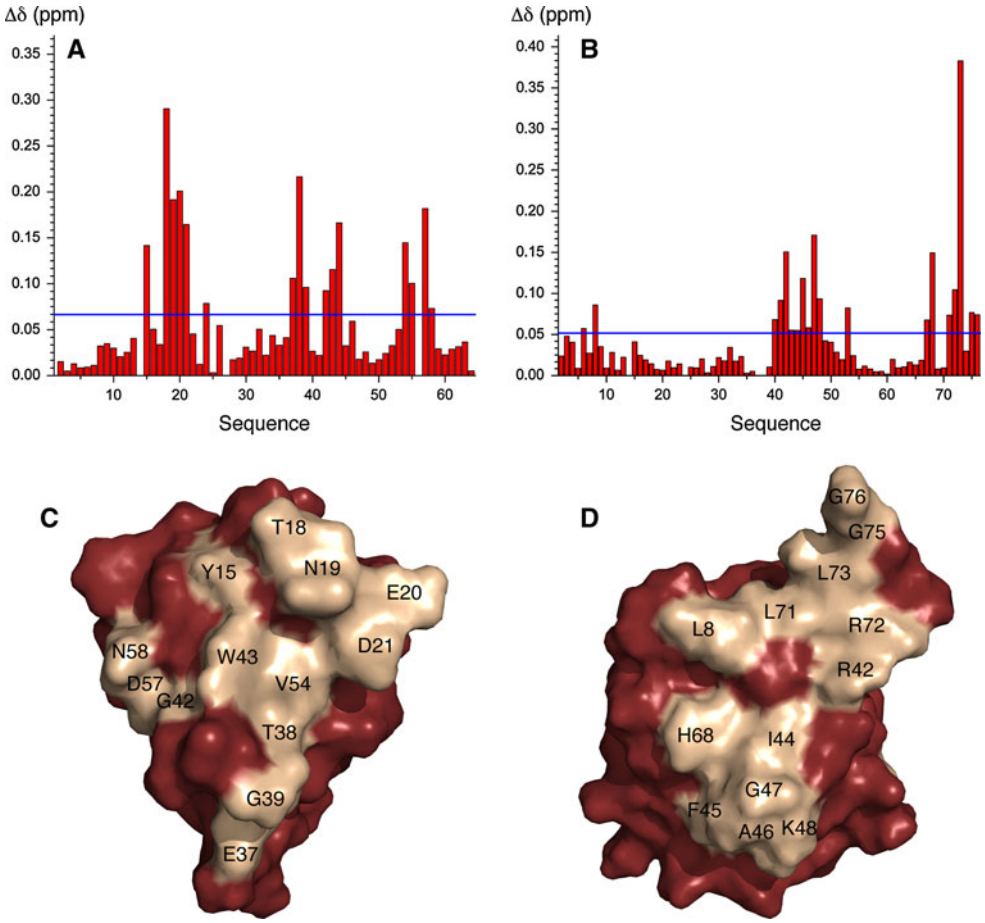

Fig. 2a–d Mapping of the complex interface between ubiquitin and SH3-C. **a**, **b** Combined chemical shift changes of ^{1}H and ^{15}N ($\Delta\delta = \sqrt{(\Delta\delta_H)^2 + (\Delta\delta_N/6.5)^2}$) in SH3-C (**a**) and ubiquitin (**b**) between the first and last titration point shown in Fig. 1a, b. The *blue solid lines* indicate the mean chemical shift changes that were used to define the residues for which ambiguous intermolecular restraints were included in HADDOCK calculations. **c**, **d** Surface representations of SH3-C (**c**) and ubiquitin (**d**) showing the location of the residues (*beige patches*) with most pronounced chemical shift changes in the titrations

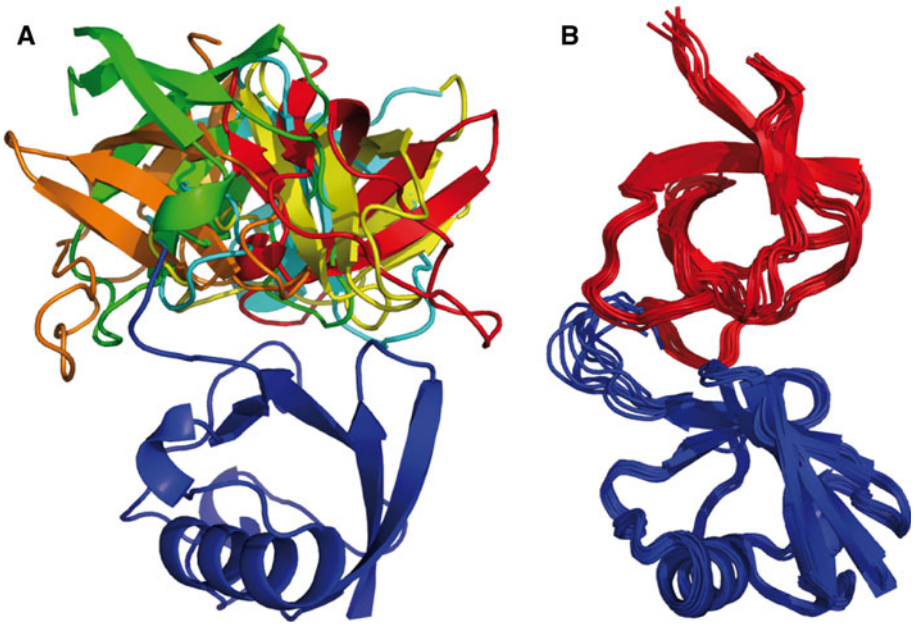

Fig. 3a, b Determination of the structure of the ubiquitin/SH3-C complex. **a** Ensemble of conformers of the ubiquitin/SH3-C complex obtained using HADDOCK fulfilling the experimental chemical shift perturbations. **b** Refined structure of the ubiquitin/SH3-C complex using experimental chemical shift perturbations and RDCs for both proteins

temperature. For example, lipid bicelles adopt anisotropic phases only at rather high temperatures (>30°C) and are restricted to a narrow pH range (~6–7), while ethylene glycol/alcohol liquid crystals can be applied at a much wider range of temperatures and pH. A second point to take into account is the type and strength of the interaction between the alignment medium and the protein of interest. For example, negatively charged filamentous phages are

not appropriate to align proteins with a high positive net charge. In general, a trial-and-error approach has to be employed where different alignment media are tested to find the most appropriate one.

The dipolar coupling can conveniently be expressed through a second rank tensor that describes the overall alignment of the molecules in the magnetic field. In the absence of internal dynamics, Eq. 1 can be recast to (Blackledge 2005):

$$D_{ij} = -\frac{\gamma_i \gamma_j \hbar \mu_0}{8\pi^2 r^3}\left[A_a(3\cos^2\theta - 1) + \frac{3}{2}A_r \sin^2\theta\cos(2\varphi)\right] \quad (3)$$

Here, A_a and A_r are the axial and rhombic components of the alignment tensor and (θ, φ) describes the orientation of the internuclear vector (e.g., N–H^N, C_α–H_α, C_α–C', and H^N–C') with respect to the alignment tensor.

RDCs have been used extensively in the determination of protein structures reporting both on local structure as well as more global features such as the relative orientation of secondary structure elements that otherwise are difficult to obtain precisely using nuclear Overhauser enhancements (NOEs) alone (Prestegard et al. 2000). However, it is worth noting that experimental RDCs possess a strong angular degeneracy meaning that a single vector has an infinite number of possible orientations for a measured RDC characterized by a given alignment tensor. This degeneracy can be raised by measuring RDCs in several different alignment media described by independent alignment tensors and/or by measuring multiple couplings for a motif of fixed geometry such as the peptide plane (Hus et al. 2008). Besides providing structural information, RDCs are sensitive to molecular motions occurring on time scales up to the millisecond. A mapping of protein motions using RDCs has been carried out in small proteins where extensive sets of RDCs have been measured in many different, independent alignment media (Meiler et al. 2001; Tolman 2002; Clore and Schwieters 2004; Bernadó and Blackledge 2004; Salmon et al. 2009; Markwick et al. 2009; Salmon et al. 2011b) and in partially folded proteins (Jensen et al. 2009). These studies have led to important discoveries regarding slow protein dynamics in solution such as the presence of slow correlated motions across β-sheets (Bouvignies et al. 2005), the role of conformational selection in molecular recognition dynamics of protein–protein complexes (Lange et al. 2008), and the nature of dynamic equilibria in partially formed molecular recognition elements (Jensen et al. 2008) and unfolded proteins (Nodet et al. 2009; Salmon et al. 2010).

RDCs are also very powerful tools for the determination of the structure of protein–protein complexes where information about the relative orientation of the two partner proteins can be obtained by superimposing their independently determined alignment tensors. The structure of the complex can be obtained by keeping the structures of the individual proteins rigid or using an approach that allows structural changes to occur in the complex in agreement with the experimentally measured RDCs. In both approaches, it is essential that the RDCs of each of the two partner proteins have been measured under saturating conditions as even small contributions to the RDCs from the unbound proteins can lead to erroneous orientations of the proteins in the complex (see below).

When can saturation be reached for a weak complex?

For a weak complex such as ubiquitin/SH3-C, it is interesting to investigate more precisely under which conditions the effective saturation of one of the proteins can be obtained without using an excessively high concentration of the partner protein (the ligand). Important factors include the propensity of proteins to aggregate or oligomerize at high concentrations such that the solubility of a protein effectively dictates the highest possible concentration in solution. The molar fraction, p_{bound}, of the protein P in a complex characterized by the dissociation constant, K_D, is given by:

$$p_{\text{bound}} = \frac{1}{2P}\left[P + L + K_D - \sqrt{(P + L + K_D)^2 - 4PL}\right] \quad (4)$$

Using a first order Taylor expansion of the square root, it can be shown that the highest possible value of p_{bound} for a given total concentration, L, of the ligand is:

$$\lim_{P\to 0} p_{\text{bound}} = \frac{L}{K_D + L} \quad (5)$$

This shows that in order to significantly populate the bound state, the ligand concentration must exceed the K_D value. As an example, we focus on a K_D of 132 μM as measured for the ubiquitin/SH3-C complex. Assuming a ligand concentration of 1 mM, the maximum p_{bound} value is 0.88. Even for very high ligand concentrations such as 5 mM, the bound state can only be populated to 97%. Therefore, it is very difficult to obtain experimental conditions where a weak complex is fully populated, and other approaches have to be used to extract structural parameters that originate from the bound, complex state alone.

Looking at Eq. 5, it is possibly surprising that weak interactions can be of any biological significance as the concentrations of the proteins in the cell are unlikely to fall in the millimolar range. It is however necessary to keep in mind that local concentrations can be quite high, due to cellular compartmentalization or due to other (stronger)

protein–protein interactions that co-localize the two partner proteins (Schreiber and Keating 2011). The CD2-associated protein contains three SH3 domains (A, B, and C) with different affinities for ubiquitin with SH3-A having the highest affinity (Ortega Roldan et al. 2011). The CD2-associated protein binds poly-ubiquitin, and the presence of several SH3 domains increases the local concentration of ubiquitin supporting the biological relevance of the weak ubiquitin/SH3-C complex.

Titration of residual dipolar couplings

In order to overcome the difficulties encountered in obtaining RDCs that emanate from the complex alone, a titration approach can be employed where RDCs are measured in different equilibrium mixtures of the free and bound form. Thus, any experimental RDC measured in an equilibrium mixture, m, of the two partner proteins is given by (Bolon et al. 1999; Lipsitz and Tjandra 2004):

$$D_{ij}^{m,\mathrm{exp}} = \lambda_m (p_{\mathrm{bound}} D_{ij}^{\mathrm{bound}} + (1 - p_{\mathrm{bound}}) D_{ij}^{\mathrm{free}}) \quad (6)$$

where D_{ij}^{free} and D_{ij}^{bound} are the RDCs in the free and bound states, respectively, and λ_m is a scaling factor that takes into account the level of alignment in the different equilibrium mixtures. While the RDCs of the free states can be measured directly, the RDCs originating from the bound state will be obtained indirectly by extrapolation of the RDCs in the different equilibrium mixtures.

The titration approach can conveniently be combined with isotope labeling schemes that allow spectroscopic filtering. For the ubiquitin/SH3-C complex, differential isotope labeling of the two partners was employed, i.e., ^{15}N-labeled ubiquitin and ^{15}N/^{13}C-labeled SH3-C. This labeling scheme allowed the measurement of different types of RDCs from the double-labeled protein in HNCO and HN(CO)CA type experiments (N–H$^{\mathrm{N}}$, C_α–H_α, C_α–C′, and C′–H$^{\mathrm{N}}$), while N–H$^{\mathrm{N}}$ RDCs were obtained of the single-labeled protein from a pair of spin-state-selected spectra where the signals of the double-labeled protein were suppressed using pulsed field gradients and phase cycling by transfer steps from ^{15}N to ^{13}C′. The advantage of this isotope labeling scheme is that RDCs are measured for both components of the complex in a given equilibrium mixture under identical alignment conditions, thereby reducing the number of mixtures required to obtain the RDCs in the complex. The same isotope labeling scheme has been proposed for the measurement of N–H$^{\mathrm{N}}$ RDCs in protein–protein complexes as the splitting between the TROSY and anti-TROSY components where the signals of the two proteins are separated into different subspectra by exploiting the presence or absence of the N–C′ scalar coupling (Bermel et al. 2009). A similar approach was used to obtain RDCs from three proteins of a ternary complex employing ^{15}N, ^{15}N/^{13}C and ^{15}N/^{13}C′, or ^{15}N/$^{13}C_\alpha$ labeling, respectively, of the three components (Tonelli et al. 2009).

RDCs were measured in three different equilibrium mixtures of SH3-C and ubiquitin giving rise to p_{bound} values of 0.79, 0.61, and 0.49 for ubiquitin and 0.44, 0.75, and 0.84 for SH3-C (Table 1). In addition, the RDCs of the free proteins were measured. To obtain coherent RDC data, the different equilibrium mixtures were prepared from the same stock solutions. In all cases, a liquid crystal composed of polyethylene glycol and 1-hexanol was employed to align the proteins. The scaling factors, λ_m, were optimized for each equilibrium mixture to take into account the different degree of alignment by ensuring linearity of the experimental RDCs versus the p_{bound} values (Table 1). The appropriate λ_m values can easily be determined because the same scaling factor applies to the RDCs of both proteins of a given equilibrium mixture where the two proteins have different p_{bound} values. As expected, the obtained scaling factors are similar to the experimental deuterium splittings measured in each of the aligned samples (Table 1). The RDCs of the complex forms of ubiquitin and SH3-C were then obtained by linear extrapolations to a p_{bound} value of 1 (Fig. 4).

Other studies have employed a similar RDC titration approach, although in a simplified version using a single equilibrium mixture, for example for determining the ligand geometry in ligand–protein complexes (Bolon et al. 1999; Koenig et al. 2002; Jain et al. 2003) and for studying protein–protein complexes with certain symmetry properties (Jain et al. 2004). Recently, the approach has been applied to resolve the structure of a weakly associated protein homodimer where RDCs were measured at three

Table 1 Equilibrium mixtures of ubiquitin and SH3-C used for extrapolation of RDCs to the bound, complex state

Equilibrium mixture	m_1	m_2	m_3	$m_{0,\mathrm{SH3}}$	$m_{0,\mathrm{UBI}}$
p_{bound} for SH3-C	0.44	0.75	0.84	0.00	–
p_{bound} for ubiquitin	0.79	0.61	0.49	–	0.00
Experimental deuterium splittings (Hz)[a]	29 (1.16)	25 (1.00)	25 ($\equiv$1)	18 (0.72)	37 (1.48)
λ_m	1.233	1.027	$\equiv$1	0.643	1.643

[a] The numbers *in parentheses* indicate the scaled deuterium splittings relative to the m_3 mixture, for comparison with λ_m values scaled to λ_3

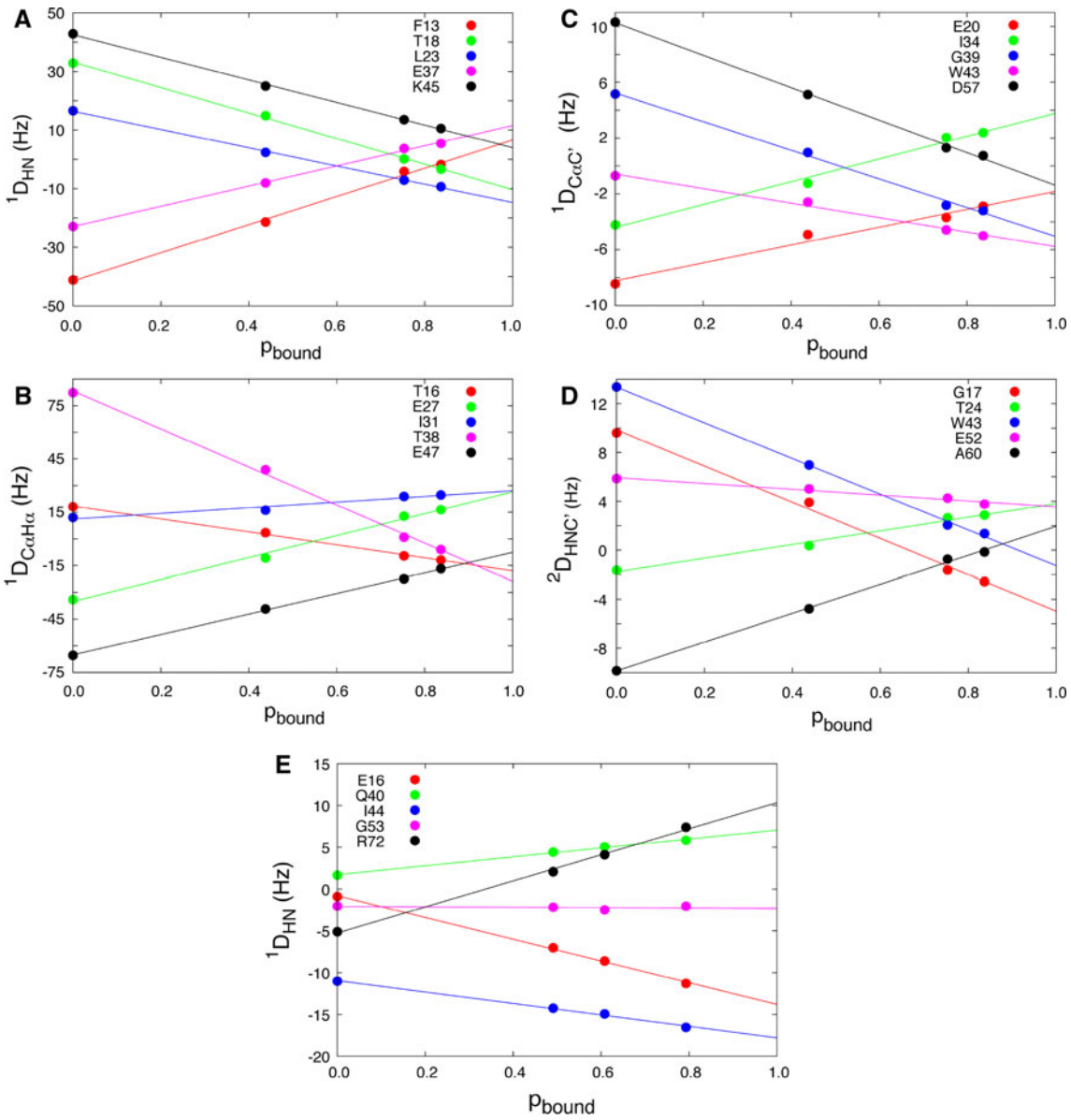

Fig. 4 Dependence of experimental RDCs (scaled with the optimized λ_m values) on the fraction p_{bound} for selected residues in SH3-C (**a–d**) and ubiquitin (**e**)

different concentrations of the protein and subsequently extrapolated to infinite concentration (Lee et al. 2010).

Determination of the structure of the complex between ubiquitin and SH3-C

The RDCs obtained by extrapolation to the fully bound form of ubiquitin and SH3-C were used to determine the relative orientation of the two proteins in the complex. The alignment tensor eigenvalues obtained from the experimental RDCs of the fully bound forms and the known structures of the isolated proteins were similar, and the structure of the complex was determined by refinement using all bound form RDCs (Fig. 3b). Although some degeneracy remained in the relative orientation of the two proteins determined by RDCs in a single alignment medium, the combination of chemical shift perturbations and RDCs raised this degeneracy.

Two other weak complexes have been determined of ubiquitin and SH3 domains using slightly different NMR approaches. The complex between ubiquitin and the third SH3 domain (SH3-3) of the yeast Sla1 protein ($K_D \sim 400$ μM at 45°C) was determined on the basis of intermolecular NOE restraints (He et al. 2007). The advantage of this approach is that intermolecular NOEs can

be measured under nonsaturating conditions provided that the lifetime of the complex is long enough. The accuracy of the structure of the complex depends on the number of NOEs that can be observed experimentally. In the case of the Sla1 complex, over 100 intermolecular NOE restraints could be measured under conditions where the complex was only saturated to 50%.

The structure of the complex between the third SH3 domain (SH3-C) of the CIN85 protein and ubiquitin (K_D ~ 171 μM at 25°C) was determined using a combination of chemical shift perturbations, RDCs, and paramagnetic relaxation enhancements (PREs) induced by an MTSL spin label attached to the C-terminal end of ubiquitin (Bezsonova et al. 2008). The complex could be populated to about 97%, and N–H^N RDCs were measured under these conditions for both proteins independently. The PREs were measured under partially saturated conditions (30%) and scaled accordingly to obtain PRE values corresponding to a fully populated complex. The PREs were converted into distance restraints and used in the structure determination of the complex together with the chemical shift perturbations and the RDCs. Notably, it has been shown using relaxation dispersion measurements that the complex formation of CIN85 SH3-C and ubiquitin does not follow a simple two-state binding model, but rather follows a three-state model involving two distinct bound conformations (Korzhnev et al. 2009). The implications of the more complicated binding mode on the determination of the structure of the complex using RDCs and PREs are not known, however, in most cases the PREs will be more sensitive to low populated alternate conformations than the RDCs. Thus, extensive measurements of PREs have been applied previously to detect encounter states in electron transfer complexes demonstrating that PREs are sensitive to states that are only transiently populated (Volkov et al. 2006, 2010a, b; Bashir et al. 2010).

The determined structures of the weak complexes between ubiquitin and the different SH3 domains (Fig. 5) are similar in terms of the binding interfaces, however some differences are observed in the relative orientation of the two proteins. Although these differences may of course reflect the different types of restraints used in the structure determination of each complex, it is interesting to note that this is compatible with the existence of different binding modes of ubiquitin across various SH3 domains (Kang et al. 2008). The biological importance of these different binding modes has yet to be investigated.

The effect of nonsaturating conditions on the structure determination of protein–protein complexes using RDCs

The importance of measuring RDCs under complete saturating conditions for the structure determination of protein–protein complexes is illustrated in Fig. 6. Data were simulated from the experimentally determined alignment tensors of free and complexed SH3-C and ubiquitin and subsequently used to determine the relative orientation of the two proteins in the complex in combination with the chemical shift perturbations. Three conditions of incomplete saturation were simulated: 90% saturation of both proteins, 80% saturation, and 70% saturation. In each case the remainder of the protein was assumed to be in its free form. As is clearly visible from Fig. 6, the relative orientation of the two proteins in the complex changes significantly compared to the complex determined under saturating conditions. For weak complexes, it is therefore advisable to apply the titration

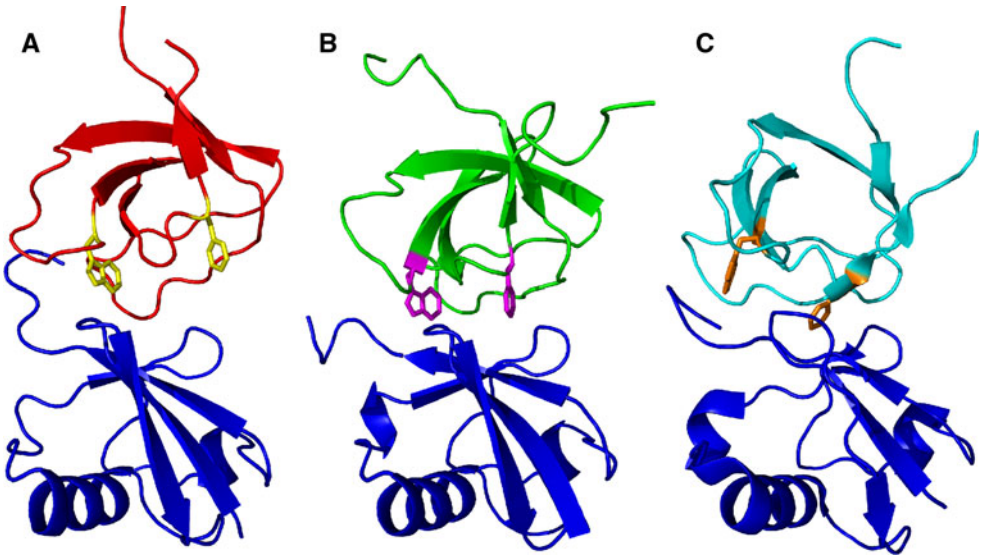

Fig. 5a–c Comparison of structures of complexes between different SH3 domains and ubiquitin: **a** CD2AP SH3-C/ubiquitin, **b** Sla1 SH3-3/ubiquitin, and **c** CIN85 SH3-C/ubiquitin. For all complexes, ubiquitin is in *blue*, while the SH3 domains have different colors. W43 and F59 in CD2AP SH3-C are shown in *yellow* sticks and the equivalent residues in Sla1 SH3-3 and CIN85 SH3-C are shown in *magenta* and *orange sticks*, respectively

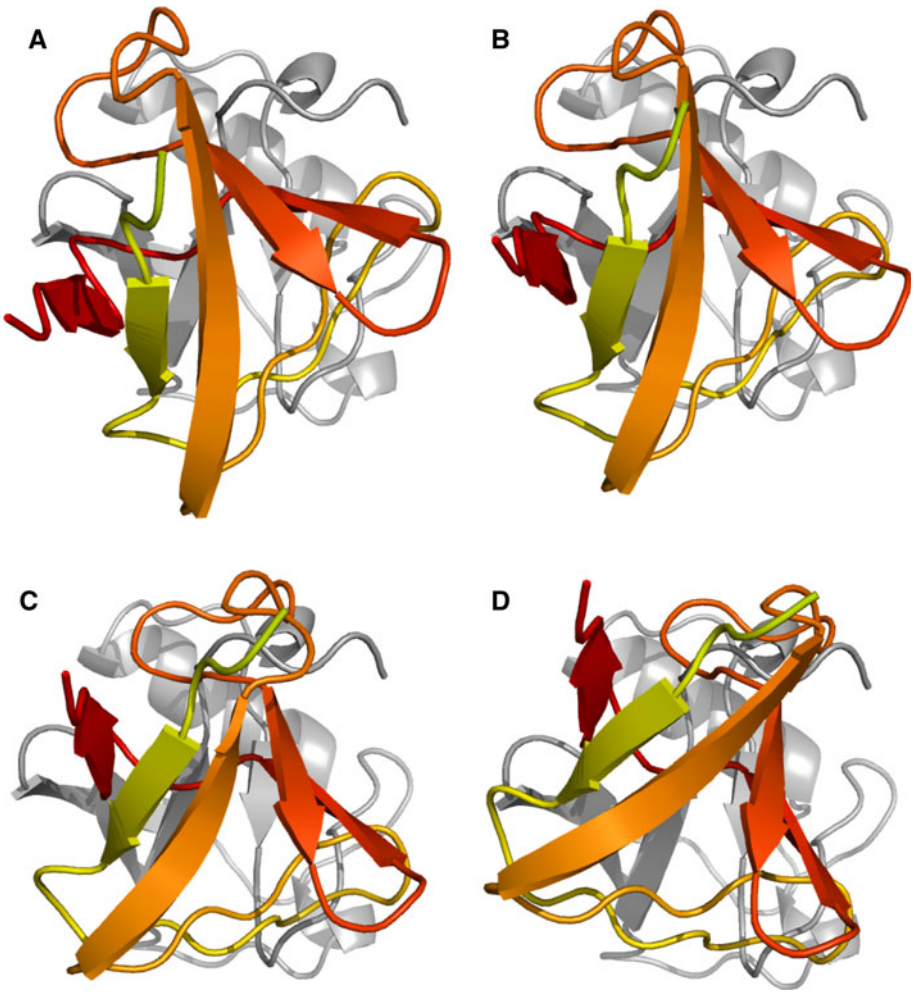

Fig. 6a–d The effect of partial saturation on the determined relative orientation of the SH3-C and ubiquitin domain. Data were simulated from the bound and free states of ubiquitin and SH3-C and mixed in ratios of 1.0:0.0 (**a**), 0.9:0.1 (**b**), 0.8:0.2 (**c**), and 0.7:0.3 (**d**). The relative orientation was determined by aligning the axes of the effective alignment tensors for the two domains

approach described above to ensure that the RDC data sets correspond to complete saturation.

Conclusions

The structural characterization of weak protein–protein complexes is not straightforward because of the difficulties in obtaining experimental parameters that report on the bound structures without contributions from the unbound, free proteins. In many cases, a titration approach is necessary where structural parameters are measured for different equilibrium mixtures of the two proteins. The present review demonstrated the application of this approach to RDCs, however, the approach can equally well be applied to other structural parameters that report on the relative orientation of the two protein domains. This includes the measurement of ^{15}N R_1 and R_2 spin relaxation rates for the determination of the overall diffusion tensor of protein–protein complexes (Salmon et al. 2011a; Lange et al. 2010) and the measurement of long-range intermolecular distance restraints exploiting paramagnetic probes attached to either of the two proteins.

References

Bashir Q et al (2010) Visualization of the encounter ensemble of the transient electron transfer complex of cytochrome c and cytochrome c peroxidase. J Am Chem Soc 132:241–247

Bax A (2003) Weak alignment offers new NMR opportunities to study protein structure and dynamics. Protein Sci 12:1–16

Bax A, Grishaev A (2005) Weak alignment NMR: a hawk-eyed view of biomolecular structure. Curr Opin Struct Biol 15:563–570

Bermel W et al (2009) Simultaneous measurement of residual dipolar couplings for proteins in complex using the isotopically discriminated NMR approach. J Am Chem Soc 131:8564–8570

Bernadó P, Blackledge M (2004) Local dynamic amplitudes on the protein backbone from dipolar couplings: toward the elucidation of slower motions in biomolecules. J Am Chem Soc 126:7760–7761

Bezsonova I et al (2008) Interactions between the three CIN85 SH3 domains and ubiquitin: implications for CIN85 ubiquitination. Biochemistry 47:8937–8949

Blackledge M (2005) Recent progress in the study of biomolecular structure and dynamics in solution from residual dipolar couplings. Prog Nucl Magn Reson Spectrosc 46:23–61

Bolon PJ, Al-Hashimi HM, Prestegard JH (1999) Residual dipolar coupling derived orientational constraints on ligand geometry in a 53 kDa protein-ligand complex. J Mol Biol 293:107–115

Bouvignies G et al (2005) Identification of slow correlated motions in proteins using residual dipolar and hydrogen-bond scalar couplings. Proc Natl Acad Sci USA 102:13885–13890

Bouvignies G, Markwick P, Brüschweiler R, Blackledge M (2006) Simultaneous determination of protein backbone structure and dynamics from residual dipolar couplings. J Am Chem Soc 128:15100–15101

Clore GM, Schwieters CD (2004) How much backbone motion in ubiquitin is required to account for dipolar coupling data measured in multiple alignment media as assessed by independent cross-validation? J Am Chem Soc 126:2923–2938

Clore GM, Starich MR, Gronenborn AM (1998) Measurement of residual dipolar couplings of macromolecules aligned in the nematic phase of a colloidal suspension of rod-shaped viruses. J Am Chem Soc 120:10571–10572

Dominguez C, Boelens R, Bonvin AMJJ (2003) HADDOCK: a protein–protein docking approach based on biochemical or biophysical information. J Am Chem Soc 125:1731–1737

Emsley JW, Lindon JC (1975) NMR spectroscopy using liquid crystal solvents. Pergamon Press, Oxford

Fielding L (2007) NMR methods for the determination of protein-ligand dissociation constants. Prog Nucl Magn Reson Spectrosc 51:219–242

Hansen MR, Mueller L, Pardi A (1998) Tunable alignment of macromolecules by filamentous phage yields dipolar coupling interactions. Nat Struct Biol 5:1065–1074

He Y, Hicke L, Radhakrishnan I (2007) Structural basis for ubiquitin recognition by SH3 domains. J Mol Biol 373:190–196

Hus J et al (2008) 16-fold degeneracy of peptide plane orientations from residual dipolar couplings: analytical treatment and implications for protein structure determination. J Am Chem Soc 130:15927–15937

Jain NU, Noble S, Prestegard JH (2003) Structural characterization of a mannose-binding protein-trimannoside complex using residual dipolar couplings. J Mol Biol 328:451–462

Jain NU et al (2004) Rapid analysis of large protein–protein complexes using NMR-derived orientational constraints: the 95 kDa complex of LpxA with acyl carrier protein. J Mol Biol 343:1379–1389

Jensen MR et al (2008) Quantitative conformational analysis of partially folded proteins from residual dipolar couplings: application to the molecular recognition element of Sendai virus nucleoprotein. J Am Chem Soc 130:8055–8061

Jensen MR et al (2009) Quantitative determination of the conformational properties of partially folded and intrinsically disordered proteins using NMR dipolar couplings. Structure 17:1169–1185

Kang J et al (2008) Distinct interactions between ubiquitin and the SH3 domains involved in immune signaling. Biochim Biophys Acta 1784:1335–1341

Koenig BW et al (2002) Structure and orientation of a G protein fragment in the receptor bound state from residual dipolar couplings. J Mol Biol 322:441–461

Korzhnev DM et al (2009) Alternate binding modes for a ubiquitin-SH3 domain interaction studied by NMR spectroscopy. J Mol Biol 386:391–405

Lange OF et al (2008) Recognition dynamics up to microseconds revealed from an RDC-derived ubiquitin ensemble in solution. Science 320:1471–1475

Lange A et al (2010) NMR reveals a different mode of binding of the Stam2 VHS domain to ubiquitin and diubiquitin. Biochemistry 50:48–62

Lee H et al (2010) Three-dimensional structure of the weakly associated protein homodimer SeR13 using RDCs and paramagnetic surface mapping. Protein Sci 19:1673–1685

Lipsitz RS, Tjandra N (2004) Residual dipolar couplings in NMR structure analysis. Annu Rev Biophys Biomol Struct 33:387–413

Markwick PRL et al (2009) Toward a unified representation of protein structural dynamics in solution. J Am Chem Soc 131:16968–16975

Meiler J et al (2001) Model-free approach to the dynamic interpretation of residual dipolar couplings in globular proteins. J Am Chem Soc 123:6098–6107

Nodet G, Salmon L, Ozenne V, Meier S, Jensen MR, Blackledge M (2009) Quantitative description of backbone conformational sampling of unfolded proteins at amino acid resolution from NMR residual dipolar couplings. J Am Chem Soc 131:17908–17918

O'Connell MR, Gamsjaeger R, Mackay JP (2009) The structural analysis of protein–protein interactions by NMR spectroscopy. Proteomics 9:5224–5232

Ortega Roldan JL et al (2007) The high resolution NMR structure of the third SH3 domain of CD2AP. J Biomol NMR 39:331–336

Ortega Roldan JL et al (2009) Accurate characterization of weak macromolecular interactions by titration of NMR residual dipolar couplings: application to the CD2AP SH3-C:ubiquitin complex. Nucleic Acids Res 37:e70

Ortega Roldan JL, Blackledge M, van Nuland NAJ, Azuaga AI (2011) Solution structure, dynamics and thermodynamics of the three SH3 domains of CD2AP. J Biomol NMR 50:103–117

Prestegard JH, al-Hashimi HM, Tolman JR (2000) NMR structures of biomolecules using field oriented media and residual dipolar couplings. Q Rev Biophys 33:371–424

Rückert M, Otting G (2000) Alignment of biological macromolecules in novel nonionic liquid crystalline media for NMR experiments. J Am Chem Soc 122:7793–7797

Salmon L et al (2009) Protein conformational flexibility from structure-free analysis of NMR dipolar couplings: quantitative and absolute determination of backbone motion in ubiquitin. Angew Chem 48:4154–4157

Salmon L et al (2010) NMR characterization of long-range order in intrinsically disordered proteins. J Am Chem Soc 132: 8407–8418

Salmon L et al (2011a) Structure, dynamics, and kinetics of weak protein–protein complexes from NMR spin relaxation measurements of titrated solutions. Angew Chem 50:3755–3759

Salmon L, Bouvignies G, Markwick P, Blackledge M (2011b) Nuclear magnetic resonance provides a quantitative description of protein conformational flexibility on physiologically important time scales. Biochemistry 50:2735–2747

Sass HJ et al (2000) Solution NMR of proteins within polyacrylamide gels: diffusional properties and residual alignment by mechanical stress or embedding of oriented purple membranes. J Biomol NMR 18:303–309

Schreiber G, Keating AE (2011) Protein binding specificity versus promiscuity. Curr Opin Struct Biol 21:50–61

Stamenova SD et al (2007) Ubiquitin binds to and regulates a subset of SH3 domains. Mol Cell 25:273–284

Takeuchi K, Wagner G (2006) NMR studies of protein interactions. Curr Opin Struct Biol 16:109–117

Tjandra N, Bax A (1997) Direct measurement of distances and angles in biomolecules by NMR in a dilute liquid crystalline medium. Science 278:1111–1114

Tolman JR (2002) A novel approach to the retrieval of structural and dynamic information from residual dipolar couplings using

several oriented media in biomolecular NMR spectroscopy. J Am Chem Soc 124:12020–12030

Tolman JR et al (1995) Nuclear magnetic dipole interactions in field-oriented proteins: information for structure determination in solution. Proc Natl Acad Sci USA 92:9279–9283

Tonelli M et al (2009) One-sample approach to determine the relative orientations of proteins in ternary and binary complexes from residual dipolar coupling measurements. J Am Chem Soc 131:14138–14139

Torbet J, Maret G (1979) Fibres of highly oriented Pf1 bacteriophage produced in a strong magnetic field. J Mol Biol 134:843–845

Tycko R, Blanco FJ, Ishii Y (2000) Alignment of biopolymers in strained gels: a new way to create detectable dipole−dipole couplings in high-resolution biomolecular NMR. J Am Chem Soc 122:9340–9341

Vaynberg J, Qin J (2006) Weak protein–protein interactions as probed by NMR spectroscopy. Trends Biotech 24:22–27

Volkov AN et al (2006) Solution structure and dynamics of the complex between cytochrome c and cytochrome c peroxidase determined by paramagnetic NMR. Proc Natl Acad Sci USA 103:18945–18950

Volkov AN, Bashir Q et al (2010a) Shifting the equilibrium between the encounter state and the specific form of a protein complex by interfacial point mutations. J Am Chem Soc 132:11487–11495

Volkov AN, Ubbink M, van Nuland NAJ (2010b) Mapping the encounter state of a transient protein complex by PRE NMR spectroscopy. J Biomol NMR 48:225–236

Zuiderweg ERP (2002) Mapping protein–protein interactions in solution by NMR spectroscopy. Biochemistry 41:1–7